In this work, the author's present an in-depth look at the gas-particle partitioning of a handful of important, highly oxygenated compounds. Uncertainty in the partitioning of these compounds, and the potential of salting-in to describe observed discrepancies is an important unanswered question that is of interest to readers of this journal. Overall, this work is technically sound and should be published. Some minor concerns and comments are described below:

Response:

Thanks for the reviewer's comments, and we'll reply these point by point.

General comments:

1. The approach to modeling partitioning nicely accounts for partitioning between phases, but a lot of the information to understand their approach is split between the SI and the main text. Some of the SI I think should maybe be brought into the main text (probably at least Eq. S1 and/or S2, and Figure S2)

Response:

Thanks. We have moved those equations and Figure S2 (now Figure 1) into the main text. To clarify the approach used for the exploration of gas-particle partitioning of polyol tracers, three partitioning cases were defined in the revised manuscript.

Pages 10-13, lines 238-295

"**Calculations of partitioning coefficients**. Here, we defined three partitioning cases to explore the influence of dissolution in aerosol liquid water on gas-particle partitioning of polyol tracers in the atmosphere. *Case 1* presumes instantaneous equilibrium between the gas phase and particulate OM based on the equilibrium absorptive partitioning theory. In this case, particulate OM is assumed to be the only absorbing phase and behave as an ideal solution. Then the absorptive gas-particle partitioning coefficients ($K_{\mathrm{p,OM}}$, m^3 μg^{-1}) were calculated from measurements ($K^{\mathrm{m}}_{\mathrm{p,OM}}$) and predicted theoretically ($K^{\mathrm{t}}_{\mathrm{p,OM}}$) as follows

$$K^{\mathrm{m}}_{\mathrm{p,OM}} = \frac{F/M_{\mathrm{OM}}}{A} \qquad (2)$$

$$K^{\mathrm{t}}_{\mathrm{p,OM}} = \frac{RT}{10^6\overline{\mathrm{MW}}_{\mathrm{OM}}\zeta_{\mathrm{OM}}p^{\mathrm{o}}{}_{\mathrm{L}}} \qquad (3)$$

where M_{OM} denotes the mass concentration of absorptive organic matter (OM = OC × 1.6; Turpin and Lim, 2001); F (ng m^{-3}) and A (ng m^{-3}) are particulate and gaseous concentrations of individual polyols, respectively. In eq 3, R (m^3 atm K^{-1} mol^{-1}) and T (K) are the ideal gas constant and ambient temperature; $\overline{\mathrm{MW}}_{\mathrm{OM}}$, average molecular weight of absorptive OM, is set at 200 g mol^{-1} for all samples (Barsanti and Pankow, 2004; Williams et al., 2010); ζ_{OM} denotes the mole fraction scale activity coefficient, and is presumed to be unity for all species in each sample; $p^{\mathrm{o}}{}_{\mathrm{L}}$ (atm) is the vapor pressure of each pure compound, and is predicted with several estimation tools and adjusted for each sampling interval based on the average temperature (Text S3 and Table S4).

Due to the influence of mixing state and water content in aerosols, several studies modeled the gas-particle partitioning of oxygenated organic compounds by defining a liquid-liquid phase separation (LLPS) in the aerosol (Zuend and Seinfeld, 2012; Pye et al., 2018). The organic-inorganic interactions and changes of activity coefficients in aqueous mixtures were fully considered as well. In this study, we proposed a simplified LLPS partitioning mechanism (*Case 2*) in Figure 1. First, aerosol water and water-insoluble OM (WIOM = OM – WSOC × 1.6) exist in two separate liquid phases, and WSOC and inorganic ions are totally dissolved in the aqueous phase. The distribution of polyol tracers between aqueous (F_{W}, ng m^{-3}) and WIOM (F_{WIOM}, ng m^{-3}) phases is simply depicted by their octanol-water partition coefficients (K_{OW})

$$K_{\mathrm{OW}} = \frac{F_{\mathrm{WIOM}}/V_{\mathrm{WSIOM}}}{F_{\mathrm{w}}/V_{\mathrm{w}}} = \frac{c_{\mathrm{WIOM}}}{c_{\mathrm{w}}} \qquad (4)$$

where V_{WIOM} and V_{w} are volumes (m^3) of WIOM and water in aerosols per cubic meter air; c_{WIOM} and c_{w} are solution concentrations (ng m^{-3}) of polyols concentrations in organic and aqueous phases; log K_{OW} values of target polyols were estimated using the Estimation Programs Interface (EPI) Suite developed by the US Environmental Protection Agency and Syracuse Research Corporation (Table S4; US EPA, 2012). The density of organic matter and water (ρ_{w}) in aerosols are set at 1.4 and 1.0 g cm^{-3}, respectively (Isaacman-VanWertz et al., 2016; Taylor et al., 2017). Second, gas-phase polyol tracers are in equilibrium with hydrophobic OM and the aqueous phase, respectively

$$K^{\mathrm{m}}_{\mathrm{p,WIOM}} = \frac{F_{\mathrm{WIOM}}/M_{\mathrm{WIOM}}}{A} \qquad (5)$$

$$K^{\mathrm{m}}_{\mathrm{H,e}} = \frac{\frac{F_W}{M_i}}{\frac{A}{M_i}\times R\times T\times\frac{c_{\mathrm{ALW}}}{\rho_{\mathrm{w}}}} = \frac{\rho_{\mathrm{w}}\times F_W}{A\times R\times T\times c_{\mathrm{ALW}}} \qquad (6)$$

where $K^{\mathrm{m}}_{\mathrm{H,e}}$ (mol m^{-3} atm^{-1}) is the measurement-based effective Henry's law coefficient; M_{WIOM} represents the mass concentration (μg m^{-3}) of WIOM; M_i (g mol^{-1}) is the molecular weight of specific compound; c_{ALW} (μg m^{-3}) is the mass concentration of aerosol liquid water predicted using ISORROPIA II model. *Case 3* is generally the same as *Case 2*, and the only difference is that water-soluble OM (WSOM) and WIOM exist in a single organic phase. Here total particulate OM was used instead of WIOM to assess the distribution of polyol tracers between aqueous and organic phases, and calculate partitioning coefficients of gas vs. particulate organic ($K^{\mathrm{m}}_{\mathrm{p,OM}}$) and aqueous ($K^{\mathrm{m}}_{\mathrm{H,e}}$) phases. Note that the polarity of particulate OM phase in *Case 3* was expected to increase, then using K_{OW} to calculate the distribution of polyols between organic and aqueous phases might lead to underestimated $K^{\mathrm{m}}_{\mathrm{p,OM}}$ and overestimated $K^{\mathrm{m}}_{\mathrm{H,e}}$. For comparison purposes, the Henry's law coefficient in pure water at 25 °C ($K^{*}_{\mathrm{H,w}}$) was estimated using EPI and SPARC (Hilal et al., 2008; http://archemcalc.com/sparc-web/calc), respectively (Table S4), and was adjusted for each sampling interval due to the changes in ambient temperature using van 't Hoff equation (Text S4). ”

2. A critical question in this work, I think, what is the uncertainty on F%? Uncertainty on these measurements is not really discussed. This parameter is calculated as the ratio of two measurements, each of which likely have at least 10-15% uncertainty (typical of GC), so there is some uncertainty on F% for any given point (though that may decrease as you get to the extreme cases of being mostly in the particle phase as in this case). That doesn't account for the uncertainty on the breakthrough which is significant (e.g., methyltetrols breakthrough is ~20+/-10%, so the correction factor for breakthrough is between a factor of roughly 1.1 and 1.3). Random error on each point should be reduced in the average (i.e., the average F% is known better than any one point), but the averages could be susceptible to systemic errors like uncertainty in breakthrough that could create bias. I do notice that during the periods of high particle concentrations for e.g., 2-MTs, F% does sometimes reach 100%, so perhaps bias is minimal, but it would be nice to get some estimates of uncertainties, or additional discussion and analysis of potential error. For instance, couldn't the divergence in Figure 2 of the isoprene tracers from the line be due to some bias like uncertainty in breakthrough?

Response:

Thanks. The measurement uncertainties will not only impact the calculation results of particle phase fractions (*F*%) of polyol tracers, but also the partitioning coefficients of gas vs. particulate organic ($K^{m}_{p,OM}$) and aqueous ($K^{m}_{H,e}$) phases.

The uncertainty estimation for measurements and partitioning coefficients were added in the revised manuscript and supplementary information, respectively.

Page 13, lines 296 – 303 of the main text:

"***Uncertainty estimation.*** To obtain the uncertainty associated with the calculation of *F*% and partitioning coefficients ($K^{m}_{p,OM}$ and $K^{m}_{H,e}$), measurement uncertainties of polyol tracers in filter and PUF samples were estimated from their recoveries and breakthrough for gaseous sampling. The root sum of squares (RSS) method was applied to propagate uncertainties of gas and particle-phase concentrations for *F*%, $K^{m}_{p,OM}$, and $K^{m}_{H,e}$ calculations. Details of the uncertainty estimation and propagation methods were provided in Text S5, and the average relative uncertainties were summarized in Table S5."

Text S5 in supplementary information:

"***Text S5. Uncertainty estimation methods***

In this work, the measurement results of some polyol tracers in filter and PUF samples are subject to substantial uncertainties due to their low and variable recoveries (Table S2) and excessive breakthrough (Figure S2). A general equation was derived to estimate measurement uncertainties of individual polyols in filter and PUF samples

$$\Delta C = \sqrt{(\text{error fraction} \times \text{concentration})^2 + (0.5 \times \text{detection limit})^2} \qquad (5)$$

where ΔC is the uncertainty of target species in filter (ΔQ_f and ΔQ_b, ng m^{-3}) or PUF (ΔPUF, ng m^{-3}) samples. The error fraction (%) of filter sample analysis was defined as half of the difference between maximum and minimum recoveries scaled by the average (Table S2), which was divided by (1 - average breakthrough) for PUF analysis (Figure S2). The average breakthrough of meso-erythritol (23.8%), mannose (38.1%), xylitol (36.4%), and arabitol (36.4%) were set as those of C5-alkene triols, glucose, and mannitol, respectively. According to the gas-particle separation method in this work, ΔQ_f was used to represent the uncertainty of particle-phase concentration (ΔF, ng m^{-3}), and the uncertainty of gas-phase concentration (ΔA, ng m^{-3}) was propagated by

$$\Delta A = \sqrt{\Delta Q_b{}^2 + \Delta \text{PUF}^2} \qquad (6)$$

Then the uncertainty of total concentration (ΔS, ng m^{-3}) was calculated as

$$\Delta S = \sqrt{\Delta F^2 + \Delta A^2} \qquad (7)$$

The uncertainties of particle-phase fractions (ΔF%) and partitioning coefficients ($K^{m}_{p,OM}$ and $K^{m}_{p,WIOM}$, m^3 ug^{-1}; $K^{m}_{H,e}$, mol m^{-3} atm^{-1}) were estimated by propagating

ΔF, ΔS, and ΔA using a simplified root sum of squares (RSS) method (Dutton et al., 2009)

$$\Delta F\%=\sqrt{(\frac{\partial F\%}{\partial F}\Delta F)^2+(\frac{\partial F\%}{\partial S}\Delta S)^2}\times 100\% \qquad (8)$$

$$\Delta K=\sqrt{(\frac{\partial K}{\partial F'}\Delta F')^2+(\frac{\partial K}{\partial A}\Delta A)^2} \qquad (9)$$

where ΔK is the uncertainty of $K^{m}_{p,OM}$, $K^{m}_{p,WIOM}$, or $K^{m}_{H,e}$; F' could be F, concentrations of polyols in WIOM (F_{WIOM}) or aqueous (F_{w}) phases, depending on the partitioning scheme (*Cases 1–3*) and partitioning coefficient for calculation. ΔF was split into ΔFw and ΔF_{WIOM} (or ΔF_{OM}) based on their ratios in eq. 4 of the main text. In Table S5, the estimated uncertainties are summarized and expressed in average ratios. As $K^{m}_{p,OM}$ and $K^{m}_{H,e}$ are all directly related to the ratio of particle- (F, ng m^{-3}) and gas-phase (A, ng m^{-3}) concentrations (eqs. 2, 4, 5, and 6 in the main text), their average $\Delta K/K$ values are the same (Table S5)."

Moreover, Figure 2 (now Figure 3 in the revised manuscript, shown below) has been changed by including the uncertainty of F% and one standard deviation of log $p^{o,*}$L derived from different estimation tools (Table S4). Because monosaccharides (e.g., fructose) and sugar alcohols (e.g., mannitol) had low and variable recoveries (Table S2) and excessive breakthrough for gaseous sampling (Figure S2), their average F% uncertainties (6.16–31.2%) are much larger than those of isoprene SOA tracers and levoglucosan (3.33–7.24%). As shown in the figure below, more than 95% of polyols with extremely low vapor pressures (< ~10^{-10} atm) are distributed into the particle phase, so their prominent uncertainties in F% are not physically meaningful. Considering the uncertainties in F% and log $p^{o,*}_{L}$ and high average F% (> 85%) of polyol tracers, a dependence of F% on the vapor pressure could not be determined.

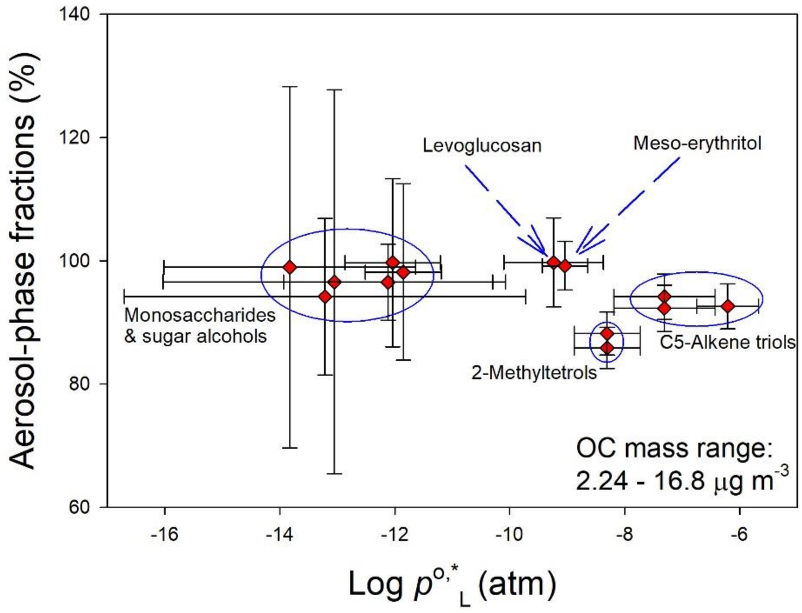

Figure 3. Average particle-phase fractions and log $p^{o,*}_{L}$ of individual polyol tracers. Whiskers represent uncertainties of F% and one standard deviation of log $p^{o,*}_{L}$ derived from different estimation tools.

In the revised manuscript, we added the above discussions on uncertainties of F% (Pages 17-18, lines 410–419).

"In Figure 3, The average *F*% uncertainties (6.16–31.2%) of monosaccharides (e.g., fructose) and sugar alcohols (e.g., mannitol) were larger than those of isoprene SOA tracers and levoglucosan (3.33–7.24%) due to their low and variable recoveries (Table S2) and excessive breakthrough (Figure S2). However, the estimated uncertainties of *F*% for less volatile polyols ($p^{o,*}_L < \sim10^{-10}$ atm) were not physically meaningful, as more than 95% of these compounds existed in the particle phase. Considering the uncertainties in *F*% and log $p^{o,*}_L$ and high average *F*% (> 85%) of target polyol tracers, a dependence of *F*% on the vapor pressure could not be determined, and the seasonality and day-night difference ($p > 0.05$) of *F*% were obscured."

3. Some of these results might be impacted by uncertainty in theoretical partitioning coefficients and by poorly constrained empirically determined coefficients.
All of the tracers shown here have values close to 100%, so there is not much dynamic range in the data and it might be susceptible to biases.
Calculation of partitioning coefficients in particular could be sensitive to uncertainties because of this (as you approach 100% in one phase, small changes in partitioning might imply large changes in K). For this reason, I'm not sure the discussion of comparison between theoretical and measured K is always that meaningful. As an extreme example, levoglucosan looks like it is always at ~100% except for maybe one point. Under these conditions, how can any meaningful K be measured, since a partitioning coefficient of 10^3 and 10^100 would both produce the same effect?
On the other hand, there is substantial error in the theoretical values as well, with uncertainty in vapor pressure likely on the order of 1-2 orders of magnitude for most of these compounds (and some evidence that EPI has a tendency to overestimate compared, see Barley and McFiggans 2010).
While I agree that the time-dependent comparisons between measured and expected K against things like sulfate (e.g., Figure 3) provide insight, comments like that on line 345 comparing measured to theoretical K quantitatively aren't that meaningful.
Similarly, if you account for these sources of uncertainty, it's not clear to me that the lines in Figure 3 necessarily have a negative intercept as described. Some discussion of these uncertainties and biases might help clarify what we do know (e.g., these tracers are mostly particle phase, theoretical vapor pressures are wrong, and correlations with absorptive theory are poor), with the quantitative aspects we don't know as well (e.g., how wrong are the vapor pressures, how strong is the dependence on salt).

Response:

In our replies to the previous two comments, we have clarified the three partitioning cases defined in this work and uncertainty estimation methods for measurements and measurement-based partitioning coefficients. To address the uncertainty of vapor pressure estimated using EPI, a variety of estimation tools were deployed to provide a reasonable vapor pressure range for each polyol tracer. Referring to Table S4 of the revised supplementary information, we can find that the vapor pressure ranges of isoprene SOA tracers, levoglucosan, and meso-erythritol are within two orders of magnitude, while those for monosaccharides and mannitol are larger (> 10^3).

The target for comparing measured and predicted partitioning coefficients is to demonstrate that particulate OM is not the only absorbing phase, and the aerosol liquid water also plays a significant role in influencing the gas-particle partitioning of polyol tracers. In Table S5 of the revised supplementary information, the average relative uncertainties of measurement-based partitioning coefficients range from a few percent to ~50%, which will result in an uncertainty of less than ± 0.3 for logarithms of partitioning coefficients. In revised Table 1, the measurement-based $K_{\mathrm{p,OM}}$ ($K^{\mathrm{m}}_{\mathrm{p,OM}}$) of isoprene SOA tracers, levoglucosan, and meso-erythritol for *Case 1* were more than 10 times greater than most theoretical predictions ($K^{\mathrm{t}}_{\mathrm{p,OM}}$). When the dissolution in aerosol liquid water was considered, their average log $K^{\mathrm{m}}_{\mathrm{p,OM}}$ became much closer to or even lay within the range (e.g., levoglucosan) of log $K^{\mathrm{t}}_{\mathrm{p,OM}}$, whenever water-soluble and water-insoluble organic matter (OM) partitioned into separate (*Cases 2*) or single (*Case 3*) liquid phases. These results support that the partitioning between gas and aerosol liquid water should not be ignored for water-soluble organic compounds like polyol tracers.

In other words, if particulate OM is the only absorbing phase in aerosols, log $K^{\mathrm{m}}_{\mathrm{p,OM}}$ values of *Case 1* will be closer to log $K^{\mathrm{t}}_{\mathrm{p,OM}}$ ranges, and the expected F% of isoprene SOA tracers, levoglucosan, and meso-erythritol should be much lower than measured in this work. To make the comparison between measured and predicted $K_{\mathrm{p,OM}}$ meaningful, we predefined three partitioning cases and estimate vapor pressures of polyol tracers using several tools, and compared average log $K^{\mathrm{m}}_{\mathrm{p,OM}}$ of different partitioning cases with log $K^{\mathrm{t}}_{\mathrm{p,OM}}$ ranges. Moreover, the $K^{\mathrm{m}}_{\mathrm{p,OM}}$ uncertainty derived from measurements was estimated and would not impact the main conclusion.

The negative intercepts shown in Figures 4 and S5 of the revised manuscript and supplements are not likely ascribed to the small relative uncertainties of partitioning coefficients (Table S5). Shen et al. (2018) also identified negative intercepts of linear regressions between log ($K_{\mathrm{H,w}}/K_{\mathrm{H,e}}$) and c_{sulfate} for glyoxal and methylglyoxal in the ambient atmosphere, and attributed this to unknown gas-particle partitioning mechanisms. By performing chamber experiments and comparing to existing laboratory studies, Kampf et al. (2013) found that the exponential increase of gas vs. aqueous phase partitioning coefficient ($K_{\mathrm{H,e}}$, mol m^{-3} atm^{-1}) with sulfate concentration only occurred at $c_{\mathrm{sulfate}} < 12$ mol kg^{-1} ALWC. In Figures 4 and S5, the log ($K_{\mathrm{H,w}}/K_{\mathrm{H,e}}$) values of most polyols increase faster as c_{sulfate} approaches 0, supporting that the enhanced uptake at low sulfate concentrations could be partly parameterized by the equation defining "salting-in" effects. However, the "salting-in" effect is a known phenomenon that is not likely linked with a specific physical or chemical mechanism. In previous studies, the increased partitioning of polar organic compounds to the particle phase was often attributed to organic-inorganic interactions, including reactive uptake, aqueous phase chemistry, etc.

In addition to the changes mentioned in previous two responses, we reorganized and rewrote the discussions on partitioning coefficients of gas versus organic and aqueous phases (*Sections 3.4 and 3.5*), considering the uncertainties in both measurements and predictions.

Pages 18-24, lines 420-560

"***3.4 Partitioning coefficients of gas versus organic phases***

To understand if particulate OM is the only absorbing phase in aerosols for polyol tracers in Nanjing, the absorptive partitioning coefficients of gas vs. organic phases were calculated based on measurement results ($K^{\mathrm{m}}_{\mathrm{p,OM}}$) for predefined *Cases*

1-3 and predicted theoretically ($K^{t}_{p,OM}$) using eq. 3 and vapor pressures listed in Table S4. In Table 1, $K^{t}_{p,OM}$ ranges of isoprene SOA tracers, levoglucosan, and meso-erythritol are within two orders of magnitude, while those of monosaccharides and mannitol are larger (> 10^{3}).When particulate OM was assumed as the only absorbing phase (*Case 1*), the average $K^{m}_{p,OM}$ of isoprene SOA tracers, levolgucosan, and meso-erythritol were more than 10 times greater than most of their $K^{t}_{p,OM}$ (Table 1), and this difference was not likely susceptible to measurement uncertainties. As shown in Table S5, the average relative uncertainties of measurement-based partitioning coefficients are all <50%, leading to an uncertainty of log $K^{m}_{p,OM}$ less than ± 0.30. Comparable or even greater (up to 10^{5}) gap between $K^{m}_{p,OM}$ and $K^{t}_{p,OM}$ has been observed for carbonyls in a number of laboratory and field studies (Healy et al., 2008; Zhao et al., 2013; Shen et al., 2018), which could be ascribed to reactive uptake (e.g., hydration, oligomerization, and esterification) of organic gases onto condensed phase (Galloway et al., 2009). Oligomers, sulfate and nitrate esters of 2-methyltetrols can be formed in the aerosol phase (Surratt et al., 2010; Lin et al., 2014), and their decomposition and hydrolysis during filter analysis will lead to an overestimation of particle-phase concentrations (Lin et al., 2013; Cui et al., 2018). However, the occurrence of oligomers, sulfate or nitrate esters of levoglucosan was not ever reported in ambient aerosols, although it can be readily oxidized by •OH in the aqueous phase of atmospheric particles (Hennigan et al., 2010; Hoffmann et al., 2010).

When solubility in aerosol liquid water was considered by assuming a LLPS in ambient aerosols, and whenever WSOM and WIOM partitioned into separate (*Case 2*) or single (*Case 3*) liquid phases, the average log $K^{m}_{p,OM}$ of the above mentioned compounds became much closer to or even lay within the range (e.g., levoglucosan) of log $K^{t}_{p,OM}$ (Table 1). These results indicated that the aerosol liquid water (21.3 ± 24.2 $\mu g\ m^{-3}$; Table S1) is also an important absorbing phase of ambient polyol tracers in Nanjing. Similarly, the measured average *F*% of isoprene SOA tracers in southeastern US and central Amazonia were higher than predictions by assuming instantaneous equilibrium between the gas phase and particulate OM only, and the agreement was improved when parameterization of solubility was included for predictions (Isaacman-VanWertz et al., 2016). But none of these two studies could reasonably predict the temporal variability of *F*% or log $K^{m}_{p,OM}$. One possible explanation is that the activity coefficients of isoprene SOA tracers and levoglucosan deviate from unity (0.42–2.04; Pye et al., 2018) and vary with PM composition. Pye et al. (2018) re-analyzed the measurement data from Isaacman-VanWertz et al. (2016) using a thermodynamic equilibrium gas-particle partitioning model in two LLPS modes, which involved organic-inorganic interactions and estimations of activity coefficients as a function of liquid PM mixture composition. The resulting predictions captured both the average and diurnal variations of measured *F*% for polyol tracers, suggesting a necessity in obtaining time-resolved activity coefficients for the implementation of absorptive equilibrium partitioning model.

……………………………………………………………………………..

3.5 Partitioning coefficients of gas versus aqueous phases

The predicted Henery's law coefficients in pure water ($K^{t}_{H,w}$, mol m^{-3} atm^{-1}) from EPI and SPARC estimates differed by several orders of magnitude, but literature values of isoprene SOA and levoglucosan were closer to EPI estimates (Table S4). If SPARC $K^{*}_{H,w}$ values were used, the average log $K^{m}_{H,e}$ of most polyol tracers would be lower than their average log $K^{t}_{H,w}$ (Table 2), indicating that the aqueous phase of ambient aerosol is less hospital to polyol tracers than pure water. This is in conflict with the fact that the interactions of organic compounds, water, and inorganic ions in aerosols will increase the partitioning of highly oxygenated compounds (O:C≥0.6; e.g., isoprene SOA tracers and levoglucosan) into the particle phase (Pye et al., 2018). Several studies identified a close relationship between salt concentrations of aerosol water and enhanced uptake of very polar compounds (Almeida et al., 1983; Kroll et al., 2005; Ip et al., 2009; Kampf et al., 2013; Shen et al., 2018). Thus, log $K^{t}_{H,w}$ values of EPI estimates were used for further data analysis.

In Table 2, the $K^{t}_{H,w}$ values of isoprene SOA tracers, levoglucosan, and meso-erythritols based on EPI estimations were 10^{2} to 10^{6} lower than their corresponding $K^{m}_{H,e}$. Log $K^{m}_{H,e}$ values of *Cases 2* and *3* had ignorable difference and were not presented separately. Other polyol compounds exhibited less difference between log $K^{m}_{H,e}$ and log $K^{t}_{H,w}$, which was very likely caused by the overestimation of their gas-phase concentrations. The average $K^{m}_{H,e}$ values of polyol tracers (10^{13}–10^{15} mol m^{-3} atm^{-1}) in this study were several orders of magnitude larger than those of carbonyls derived from ambient measurements (10^{10}–10^{12} mol m^{-3} atm^{-1}; Shen et al., 2018) and chamber simulations (~10^{11} mol m^{-3} atm^{-1}; Kroll et al., 2005; Volkamer et al., 2006; Galloway et al., 2009). This is because low molecular weight carbonyls (e.g., glyoxal) are much more volatile ($p^{o,*}_{L} > 10^{-2}$ atm) than our target polyols (Table S4). According to existing studies, the minimum concentrations of gas-phase glyoxal and methylglyoxal in Chinese cities (~0.1 µg m^{-3}) are magnitudes higher than the averages of polyol tracers in this work, while their particle-phase concentrations are of the same magnitude (Shen et al., 2018; Liu et al., 2020).

A number of previous studies observed enhanced $K_{H,e}$ of carbonyls with salt concentrations in aqueous solution (Ip et al., 2009; Kampf et al., 2013; Waxman et al., 2015; Shen et al., 2018), and described this “salting-in” effect using

$$\mathrm{Log}\left(\frac{K_{\mathrm{H,w}}}{K_{\mathrm{H,e}}}\right) = K_{\mathrm{s}} c_{\mathrm{salt}} \qquad (7)$$

where K_s (kg mol^{-1}) is the salting constant, and c_{salt} is the aqueous-phase concentration of salt in mol kg^{-1} ALWC. This equation is originally defined in Setschenow (1889) by plotting log ($K_{H,w}/K_{H,e}$) versus the total salt concentration (mol L^{-1}).

As sulfate has been identified as the major factor influencing the salting effect of carbonyl species (Kroll et al., 2005; Ip et al., 2009), Figure 4 shows modified Setschenow plots for C5-alkene triols, 2-methyltetrols, and levoglucosan, where log ($K^{t}_{H,w}/K^{m}_{H,e}$) values were regressed to the molality of sulfate ion in aerosol liquid water ($c_{sulfate}$, mol kg^{-1} ALWC). The log ($K^{t}_{H,w}/K^{m}_{H,e}$) data increased faster when $c_{sulfate}$ approached 0, and deviated from their expected behavior with increased $c_{sulfate}$. Kampf et al. (2013) selected a threshold $c_{sulfate}$ of 12 mol kg^{-1} ALWC to illustrate the deviation for chamber experiments, and attributed it to elevated viscosity and slow particle-phase reactions at high $c_{sulfate}$. In Figure 4, negative correlations ($p < 0.01$) are observed at $c_{sulfate} < 12$ mol kg^{-1} ALWC, and Figure S5 exhibits significant negative correlations ($p < 0.01$) between log ($K^{t}_{H,w}/K^{m}_{H,e}$) and $c_{sulfate}$ for individual polyols even without excluding the deviations at high $c_{sulfate}$. The K_s values of polyol tracers from Figures 4 and S5 (-0.17 – -0.037 kg mol^{-1}) are in a similar range as that of glyoxal (-0.24 – -0.04 kg mol^{-1}; Kampf et al., 2013; Shen et al., 2018; Waxman et al., 2015). These results indicated that the shifting of gas-particle equilibrium toward the condensed phase might be partly parameterized by the equation defining “salting-in” effects.

However, the “salting-in” effect is a known phenomenon that is not likely linked with a specific physical or chemical mechanism. Quantum chemical calculation results indicated negative Gibbs free energy of water displacement for interactions between SO_4^{2-} and glyoxal monohydrate (Waxman et al., 2015). The net “salting-in” effect of 1-nitro-2-naphthol in NaF solution was interpreted by postulating hydrogen bonding (Almeida et al., 1983). A direct binding of cations to ether oxygens was proposed to be responsible for the increased solubility of water-soluble polymers (Sadeghi and Jahani, 2012). Due to the moderate correlations and negative intercepts in Figures 4 and S5, the gap between $K^{t}_{H,e}$ and $K^{m}_{H,w}$ cannot be closed by the "salting-in" effect alone. Shen et al. (2018) also obtained negative intercepts when plotting log ($K^{t}_{H,w}/K^{m}_{H,e}$) over $c_{sulfate}$ for glyoxal and methylglyoxal in ambient atmosphere, and attributed this to unknown gas-particle partitioning mechanisms. Evidences showing that the thermal degradation of less volatile oligomers and organosulfates can lead to an overestimation of 2-methyltetrols by 60–188% when using a conventional GC/EI-MS method (Cui et al., 2018). To fit the gas-particle distribution of 2-methyltetrols in southeastern US, 50% of particulate 2-methyltetrols was presumed to exist in chemical forms with much lower vapor pressures by Pye et al. (2018). So, the reactive uptake and aqueous phase chemistry could be explanations for the enhanced uptake of isoprene SOA tracers. Moreover, log ($K^{t}_{H,w}/K^{m}_{H,e}$) values of polyol tracers also negatively correlated with the aqueous-phase concentrations of WSOC (c_{WSOC}, Figure S6), but not NH_4^+ or NO_3^-. This dependence might be associated with the "like-dissolves-like" rule, or indicate the importance of aqueous-phase heterogeneous reactions (Hennigan et al., 2009; Volkamer et al., 2009). Although several studies have estimated Henry's law constants for a variety of polar organic compounds in pure water (e.g., polyols and polyacids; Compernolle and Müller, 2014a, b), more work is warranted to decrease the estimation uncertainty and explain their increased partitioning toward aerosol liquid water explicitly."

Specific comments:

4. Line 57: Typo, "Filed" should say "Field"

Response:

It has been revised as suggested. (Page 4, line 80)

5. Line 85: Probably also worth mentioning that Yatavelli et al. (2014, 10.5194/acp-14-1527-2014) and Isaacman-VanWertz et al. (2016) also found good agreement with theory for alkanoic acids

Response:

The two references were added, and the original expression has been changed into

"Unlike non-polar species (e.g., *n*-alkanes, polycyclic aromatic hydrocarbons) and alkanoic acids that are well simulated (Simcik et al., 1998; Xie et al., 2014a; Yatavelli et al., 2014; Isaacman-VanWertz et al., 2016), particle-phase concentrations of carbonyls were underestimated by several orders of magnitude when particulate OM is presumed as the only absorbing phase in ideal condition (Healy et al., 2008; Kampf et al., 2013; Shen et al., 2018)." (Page 5, 109-114)

6. Line 90: Typo, "every" should say "very"

Response:

It has been revised as suggested. (Page 5, line 117)

7. Line 176: When quantifying the isoprene tracers using meso-erythritol, I assume the effect of fragmentation on the quant ion was accounted for, but that is not clear here or in the supplmental. In other words, while m/z 219 is used for the 2-MTs, something different, likely m/z 217, is used for meso-erythritol, and the fraction of total signal that is the quant ion could be different - if this was corrected for it should be stated at least in the SI, if not it should be justified.

Response:

In the current work, we did not consider the effect of fragmentation on the quant ion due to the following reasons:

(1) Meso-erythritol and isoprene tracers (C5-alkene triols and 2-methyltetrols) should have different total ion signal intensity for the same amount, so the calibration curve of meso-erythritol is expected to differ from isoprene tracers. Even if the effect of fragmentation on the quant ion was accounted for, the quantification accuracy might not be improved. A number of previous studies used meso-erythritol as surrogate for isoprene tracers without considering the effect of fragmentation (Claeys et al., 2004; Hu et al., 2008; Ding et al., 2008, 2012; Lin et al., 2013; Xie et al., 2014). It should also be noted that ketopenic acid was used to quantify all SOA tracers by Kleindienst et al. (2007).

(2) The present study focused on the gas-particle partitioning of polyol tracers. Their particle-phase fractions, measurement-based partitioning coefficients of gas versus organic ($K^{m}_{p,OM}$) and aqueous ($K^{m}_{H,e}$) phases were all directly related to the ratio of particle- to gas-phase concentrations, which is not impacted by the effect of fragmentation.

(3) The total ion peaks corresponding to isoprene tracers in ambient air samples usually combined with other compounds, thus the quant ions (m/z 219) fractions of 2-methyltetrols in total ion signal (0.14 ± 0.035, 0.20 ± 0.015) had larger variability than that of meso-erythritol (0.12 ± 0.0039), then the correction for fragmentation effect might introduce new uncertainty.

In the revised supplementary information, we added some justifications for not correcting the fragmentation effect.

"Meso-erythritol and isoprene SOA tracers were expected to have different total ion intensity for the same amount, and the total ion signals of isoprene tracers in ambient air sample often co-eluted with other compounds, so the fragmentation difference between quantification ions of meso-erythritol (m/z 217) and isoprene SOA tracers (m/z 219) was not adjusted in this work. It should be noted that meso-erythritol was used as the surrogate for isoprene tracers without considering the fragmentation effect in a number of previous studies (Claeys et al., 2004; Hu et al., 2008; Ding et al., 2008, 2012; Lin et al., 2013; Xie et al., 2014)."

8. Line 197: If gas-phase mass is being taken as Qb plus PUF, what is the purpose of the Qb measurement at all? Why not just do Qf backed by a PUF?

Response:

The backup quartz fiber filter was typically used to assess positive sampling artifact of particulate OC due to gaseous adsorption (Chow et al., 2010; Subramanian et al., 2004). In a companion study to this work, concentrations of bulk species in $PM_{2.5}$ were determined by subtracting measurement results of Q_b from Q_f (Yang et al., 2021). This has been mentioned in section 2.2 of the manuscript (Pages 8, lines 176-178).

Concentrations of polyol tracers detected on Q_b reflected filter-based sampling artifacts, which is ascribed to gaseous adsorption ("positive artifact") and evaporation loss from particles on Q_f ("negative artifact"). If polyol tracers on Q_b account for significant fractions of their total concentrations, then the separation of their particle- and gas-phase concentrations will depend largely on sampling artifact corrections. In the current work, polyol tracers were predominantly observed on Q_f with averages 1-3 orders of magnitude higher than those on Q_b and PUF, and it would be safe to assume that Q_b values were equally contributed by positive and negative artifacts. So, Q_b measurement is necessary in determining the magnitude of sampling artifacts.

The original expressions have been revised (Pages 9-10, lines 218-229).

"Polyol tracers detected in Q_b samples are contributed by both gaseous adsorption ("positive artifact") and particle-phase evaporation from Q_f samples ("negative artifact"), but their relative contributions are unknown. Xie et al. (2014b) adjusted particle- and gas-phase concentrations of levoglucosan and 2-methyltetrol based on Q_b measurements in two different ways. One assumed that Q_b values were completely attributed to gaseous adsorption; the other presumed equal contributions from gaseous adsorption and Q_f evaporation. However, negligible difference in gas-particle distribution was observed due to the small Q_b values. In Table S3, concentrations of polyol tracers on Q_b are far below those on Q_f, and it would be safe to presume equal positive and negative artifacts. In this study, particle-phase concentrations of polyols were represented by Q_f values, and the gas phase was calculated as the sum of Q_b and PUF measurements."

9. Line 220-225: I'm not completely clear on the partitioning approach. The Kow is used to partition the particle fraction between condensed phases - is this information then used in the gase-particle partitioning? For instance, is K_OM used for the organic component, and K_H used for the aqueous? I guess I'm just not clear on how Kow fits into the scheme.

Response:

Yes, the K_{OW} is used to calculate concentrations of polyol tracers in two separate aerosol phases (organic and aqueous). $K_{p,OM}$ and K_H represent gas-particle partitioning coefficients of gas versus organic and aqueous phases, respectively.

To make it clear, we defined three partitioning cases, and elucidate the calculation methods for the two partitioning coefficients in the revised manuscript.

Pages 10-13, lines 238-295 (See responses to *Comment 1*, eqs 4, 5, and 6)

10. Line 297-298: Isaacman-VanWertz et al. (2016) also show hourly diurnal profiles with a daytime high, it is interesting to see in this work that the difference between daytime and nighttime values was not significant. As noted later in the manuscript, in the summer when there are actually strong concentrations of these compounds, there is a strong diurnal, so I'm not sure it really makes sense to claim here there is no diurnal.

Response:

Similar to the observations by Fu and Kawamura (2011) at a forest site in Hokkaido, Japan, concentrations of isoprene SOA tracers in southeastern US and central Amazonia also exhibited peak concentrations from late afternoon to mid night. In the current work, daytime and nighttime samples were collected during 8:00 AM – 7:00 PM and 7:00 PM – 7:00 AM (next day), respectively. Neither the daytime or nighttime sample covered the whole period when isoprene SOA had peak concentrations. This explains why the strong diurnal variations of isoprene SOA tracers were not captured in this work.

The original expression was changed into

"Previous field studies observed strong diurnal variations of isoprene SOA tracers with peak concentrations from afternoon till midnight (Fu and Kawamura, 2011; Isaacman-VanWertz et al., 2016). Although no IEPOX will be generated from the oxidation of isoprene by •OH and HO_2• after sunset, the formations of C5-alkene triols and 2-methyltetrols might continue until pre-existing IEPOX is exhausted. In this work, neither the daytime (8:00 AM–7:00 PM) or night-time (7:00 AM–7:00 AM next day) sample covered the whole period when isoprene SOA tracers had peak concentrations, and the strong diurnal variations of C5-alkene triols and 2-methyltetrols were not captured." (Page 16, 367-375)

11. Line 336: This is the first place F% is given any error or range, though I assume here the uncertainty is the standard deviation.

Response:

We clarified in the revised manuscript that the numbers here represented ranges of average ± standard deviation. (Page 17, lines 405)

Moreover, measurement uncertainties and their influences on *F*% and partitioning coefficients were estimated in the revised manuscript. (Text S5 and Figure 3, see responses to *Comment 2*; Table S5, shown below)

Table S5. Average relative uncertainties of measurements and calculated parameters.

Species	Δ*F*/*F*[a]	Δ*A*/*A*[b]	Δ*S*/*S*[c]	Δ*F*%/*F*%[d]	Δ*K*/*K*[e]
Isoprene SOA tracers					
C5-alkene triol 1	0.028	0.032	0.027	0.037	0.043
C5-alkene triol 2	0.028	0.054	0.033	0.036	0.059
C5-alkene triol 3	0.028	0.077	0.034	0.038	0.084
2-Methylthreitol	0.028	0.051	0.028	0.033	0.059
2-Methylerythritol	0.028	0.066	0.030	0.035	0.072
Biomass burning tracer					
Levoglucosan	0.051	0.16	0.054	0.072	0.17
Sugars ang sugar alcohols					
Meso-erythritol	0.028	0.11	0.028	0.040	0.12
Fructose	0.23	0.27	0.26	0.31	0.36
Mannose	0.045	0.27	0.049	0.062	0.28
Glucose	0.094	0.28	0.10	0.18	0.31
Xylitol	0.10	0.12	0.10	0.14	0.16
Arabitol	0.097	0.26	0.099	0.14	0.28
Mannitol	0.21	0.42	0.21	0.29	0.47

[a] Particle-phase concentration; [b] gas-phase concentration; [c] total concentration; [d] particle-phase fraction; [e] partitioning coefficients of gas vs. organic and aqueous phases.

12. Line 370: This could also be due to some systematic bias in how EPI estimates vapor pressures. This might be reconcile by testing other vapor pressure estimation methods. For example EVAPORATION agrees with EPI on the vapor pressure of erythritol (log vp (atm) = ~ -8.2-8.5) but EPI estimates mannose to be two orders of magnitude more volatile (log vp (atm) = -9.5) than EVAPORATION estimates (log vp (atm) = -11.5). This also highlights the uncertainty of using comparisons against theoretical K to draw conclusions.

Response:

To address the concern on uncertainties of vapor pressures, other estimation tools were tested (Table S4). The revised Table 1 (shown below) compared measurement-based log $K_{\mathrm{p,OM}}$ of predefined *Cases 1-3* and theoretical predictions based on different vapor pressure estimation methods. Then the discussions on comparisons between measured and predicted $K_{\mathrm{p,OM}}$ were revised accordingly (Section 3.4, see responses to *Comment 3*; pages 18-20, lines 420-480).

As shown in Table 1, when the solubility in aerosol liquid water is considered (*Cases 2* and *3*), the agreement between log $K^{\mathrm{m}}_{\mathrm{p,OM}}$ and log $K^{\mathrm{t}}_{\mathrm{p,OM}}$ for isoprene SOA tracers and levoglucosan has been improved substantially. While the deviations of log $K^{\mathrm{m}}_{\mathrm{p,OM}}$ versus log $K^{\mathrm{t}}_{\mathrm{p,OM}}$ for monosaccharides and sugar alcohols became larger. This is expected to be caused by the overestimations of their gas phase concentrations due to sampling artifacts, since the vapor pressures of sugar polyols were orders of magnitude lower than isoprene SOA tracers and levoglucosan.

Table 1. Comparisons of measurement-based log $K_{p,OM}$ ($m^3\ \mu g^{-1}$) at three proposed cases and predicted values.

Species	No. of obs.	Log $K^m_{p,OM}$ [a]			Log $K^t_{p,OM}$ [b]			
		Case 1	Case 2	Case 3	EPI	EVAPORATION	SPARC	SIMPOL
Isoprene SOA tracers								
C5-alkene triol 1	53	0.33 ± 0.71	-0.79 ± 0.86	-0.82 ± 0.85	-3.09	-2.84	-1.19	-2.88
C5-alkene triol 2	63	0.15 ± 0.55	-1.02 ± 0.74	-1.05 ± 0.73	-3.62	-3.67	-4.14	-2.85
C5-alkene triol 3	83	0.35 ± 0.68	-0.83 ± 0.86	-0.86 ± 0.85	-2.90	-2.65	-1.00	-2.69
2-Methylthreitol	101	-0.12 ± 0.48	-2.09 ± 0.71	-2.09 ± 0.70	-1.87	-1.30	-1.18	-0.47
2-Methylerythritol	95	-0.011 ± 0.58	-1.96 ± 0.71	-1.96 ± 0.71	-1.90	-1.34	-1.22	-0.50
Biomass burning tracer								
Levoglucosan	65	2.23 ± 0.72	0.63 ± 0.90	0.62 ± 0.90	-0.04	-0.81	1.04	-0.76
Sugars ang sugar alcohols								
Meso-erythritol	31	0.87 ± 0.53	-1.43 ± 0.60	-1.43 ± 0.60	-0.65	-1.21	-0.45	
Fructose	85	0.65 ± 0.73	-1.20 ± 0.83	-1.20 ± 0.89	1.17	2.76	6.94	
Mannose	74	0.62 ± 0.71	-2.12 ± 0.95	-2.12 ± 0.95	1.28	2.13	4.77	
Glucose	88	0.42 ± 0.67	-2.77 ± 0.93	-2.77 ± 0.93	0.34	3.75	7.32	
Xylitol	22	0.24 ± 0.54	-2.61 ± 0.72	-2.61 ± 0.72	3.37	2.34	3.57	
Arabitol	30	1.46 ± 0.89	-1.35 ± 1.24	-1.35 ± 1.24	3.25	1.67	2.90	
Manitol	65	1.08 ± 0.63	-2.24 ± 0.95	-2.24 ± 0.95	2.33	4.16	6.68	

[a] Average ± standard deviation; [b] temperature range: -4~36 °C.

13. Line 391: Here and throughout, why use K_H,e and K_H,w for measured and predicted, respectively, for Henry's law, but K_p^m and K_p^t or measured and predicted, respectively, for absorptive partitioning. I think the discussion would be more clear if notation were more consistent (e.g, K_H^m and K_H^t

Response:

Thanks. To make it more clear and consistent, $K_{H,e}$ and $K_{H,w}$ were changed into $K^m_{H,e}$ and $K^t_{H,w}$ if necessary throughout the manuscript.

14. Line 407: out of curiosity, why did the authors choose to switch to molality instead of molarity?

Response:

The switch from molarity to molality will not influence the correlation between log ($K_{H,w}/K_{H,e}$) and sulfate concentrations. It also makes it easier to compare the salting constant (K_s) with previous studies (Kampf et al., 2013; Waxman et al., 2015; Shen et al., 2018).

References

Chow, J. C., Watson, J. G., Chen, L. W. A., Rice, J., and Frank, N. H.: Quantification of PM2.5 organic carbon sampling artifacts in US networks, Atmos. Chem. Phys., 10, 5223-5239, 10.5194/acp-10-5223-2010, 2010.

Claeys, M., Graham, B., Vas, G., Wang, W., Vermeylen, R., Pashynska, V., Cafmeyer, J., Guyon, P., Andreae, M. O., Artaxo, P., and Maenhaut, W.: Formation of secondary organic aerosols through photooxidation of isoprene, Science, 303, 1173-1176, 10.1126/science.1092805, 2004.

Ding, X., Zheng, M., Yu, L., Zhang, X., Weber, R. J., Yan, B., Russell, A. G., Edgerton, E. S., and Wang, X.: Spatial and seasonal trends in biogenic secondary organic aerosol tracers and water-soluble organic carbon in the Southeastern United States, Environ. Sci. Technol., 42, 5171-5176, 10.1021/es7032636, 2008.

Ding, X., Wang, X.-M., Gao, B., Fu, X.-X., He, Q.-F., Zhao, X.-Y., Yu, J.-Z., and Zheng, M.: Tracer-based estimation of secondary organic carbon in the Pearl River Delta, south China, J. Geophys. Res. Atmos., 117, D05313, 10.1029/2011jd016596, 2012.

Hu, D., Bian, Q., Li, T. W. Y., Lau, A. K. H., and Yu, J. Z.: Contributions of isoprene, monoterpenes, β-caryophyllene, and toluene to secondary organic aerosols in Hong Kong during the summer of 2006, J. Geophys. Res. Atmos., 113, D22206, 10.1029/2008jd010437, 2008.

Kleindienst, T. E., Jaoui, M., Lewandowski, M., Offenberg, J. H., Lewis, C. W., Bhave, P. V., and Edney, E. O.: Estimates of the contributions of biogenic and anthropogenic hydrocarbons to secondary organic aerosol at a southeastern US location, Atmos. Environ., 41, 8288-8300, 10.1016/j.atmosenv.2007.06.045, 2007.

Kampf, C. J., Waxman, E. M., Slowik, J. G., Dommen, J., Pfaffenberger, L., Praplan, A. P., Prévôt, A. S. H., Baltensperger, U., Hoffmann, T., and Volkamer, R.: Effective Henry’s law partitioning and the salting constant of glyoxal in aerosols containing sulfate, Environ. Sci. Technol., 47, 4236-4244, 10.1021/es400083d, 2013.

Lin, Y. H., Knipping, E. M., Edgerton, E. S., Shaw, S. L., and Surratt, J. D.: Investigating the influences of SO2 and NH3 levels on isoprene-derived secondary organic aerosol formation using conditional sampling approaches, Atmos. Chem. Phys., 13, 8457-8470, 10.5194/acp-13-8457-2013, 2013.

Shen, H., Chen, Z., Li, H., Qian, X., Qin, X., and Shi, W.: Gas-particle partitioning of carbonyl compounds in the ambient atmosphere, Environ. Sci. Technol., 52, 10997-11006, 10.1021/acs.est.8b01882, 2018.

Subramanian, R., Khlystov, A. Y., Cabada, J. C., and Robinson, A. L.: Positive and negative artifacts in particulate organic carbon measurements with denuded and undenuded sampler configurations special issue of aerosol science and technology on findings from the fine particulate matter supersites program, Aerosol Sci. Tech., 38, 27-48, 10.1080/02786820390229354, 2004.

Waxman, E. M., Elm, J., Kurtén, T., Mikkelsen, K. V., Ziemann, P. J., and Volkamer, R.: Glyoxal and methylglyoxal Setschenow salting constants in sulfate, nitrate, and chloride solutions: Measurements and Gibbs energies, Environ. Sci. Technol., 49, 11500-11508, 10.1021/acs.est.5b02782, 2015.

Xie, M., Hannigan, M. P., and Barsanti, K. C.: Gas/particle partitioning of 2-methyltetrols and levoglucosan at an urban site in Denver, Environ. Sci. Technol., 48, 2835-2842, 10.1021/es405356n, 2014.

Yang, L., Shang, Y., Hannigan, M. P., Zhu, R., Wang, Q. g., Qin, C., and Xie, M.: Collocated speciation of PM2.5 using tandem quartz filters in northern nanjing, China: Sampling artifacts and measurement uncertainty, Atmos. Environ., 246, 118066, https://doi.org/10.1016/j.atmosenv.2020.118066, 2021.